ARTICLE

Cross-Correlated Humidity Dependent Structural Evolution of Nafion Thin Film Confined on Platinum Substrate

Received 00th January 20xx,
Accepted 00th January 20xx

DOI: 10.1039/x0xx00000x

Udit N. Shrivastava[a], Kota Suetsugu[b], Shusaku Nagano[c], Helmut Fritzsche[d], Yuki Nagao[e], Kunal Karan[a,*]

Nanometer thin films of Nafion ionomer interfacing with platinum form the functional electrode in many electrochemical devices including fuel cells and electrolyzers. To impart facile proton conduction in Nafion ionomer, sufficient hydration of Nafion ionomer is necessary to create a percolating network of water-filled nanometer sized hydrophilic domains that manifests as macroscopic swelling. This hydration behavior of ionomer thin films is poorly understood especially for films confined on electrochemically relevant Pt substrates. In this work, we present the evolution of hydration-dependent microscopic hydrophilic domains and macroscopic expansion of 55 nm thin Nafion film on a Pt substrate. The cross-correlation among the film macro-expansion from ellipsometry, the micro-expansion from GISAXS, and the water distribution from neutron reflectometry (NR), explains the observed non-affine behavior of the film which can be attributed to the randomly and spatially non-uniform distribution of water domains. A correlation between macroscopic factor (ε/τ) for protonic conductivity, and the domain size and swelling is presented for the first time. In addition, interfacial water between Pt and the ionomer interface estimated at 75% and 84% RH, and increase in domain size with RH, are discussed to explain increased activity and oxygen diffusivity with RH.

I. Introduction

Thin Nafion films are of technological importance to polymer electrolyte based electrochemical devices such as fuel cells, electrolyzers, and sensors [1-5]. In the electrodes of these devices, sub-micron thin Nafion films coat the electron-conducting surface of the catalysts such as Pt to form an electroactive interface where their key function is to facilitate proton transport [6-9]. In addition, in the electrodes comprising ionomer-covered platinum, the reactants or analytes have to be transported through the ionomer films. Thus, the ionomer film controls both the local ion conduction and the reactant transport through the film and to/from the electrochemical interface and influence electrochemical performance parameter such as active area utilization and catalyst activity [10-11]. It is well known that the ionomer transport properties are a strong function of relative humidity (RH), which is a controllable operational parameter [12-13]. Pertinent to fuel cells, a recent study from Morimoto's group at Toyota Central R&D has demonstrated that the critically important transport resistances, viz., the oxygen diffusion resistance across the Nafion thin film and the interfacial resistance at the buried interface (i.e. at the Pt/ionomer interface), decreases significantly with RH [14]. These hydration-dependent transport properties are a manifestation of a key microscopic structural feature of these ionomers – the hydrophilic ionic domains formed by clustering of the sulphonic acid (SO3- H+) ion-pairs distributed in the hydrophobic fluorocarbon matrix. In fact, much of the research on the structure of the membrane form of Nafion has been focused on the size/shape of these ionic domains using small angle x-ray scattering (SAXS) studies [12-13].

However, thin films are fundamentally different than bulk membranes due to the confinement effects and the interfacial interaction induced orientation of ionomer chains resulting in anisotropic structures and properties [15-16]. The literature on Nafion thin films on SiO2 has provided sufficient evidence of thickness-dependent water uptake, proton conductivity, ionomer wettability, modulus of elasticity, thermal expansion and micro-to-macro relationship (local domain size-to-hygro-expansion) [17-27]. In addition to confinement, interaction with a substrate can strongly influence the structure of thin films resulting in substrate-dependent macroscopic and microscopic properties [28-34]. For example, substrate-dependent layered morphology and orientation of hydrophilic domains within hydrophilic domains have been observed from scattering techniques such as neutron reflectometry (NR) and grazing incidence small angle x-ray scattering (GISAXS) [30-34]. Substrate-dependent macroscopic properties such as water uptake kinetics, proton conductivity, and thermal expansion of the films have also been reported [24-25, 34]. Macroscopic properties of ionomer thin films on Pt such as proton conductivity, and the microscopic structure such as water distribution and ordering of hydrophilic domains greatly differs from the ionomer thin film on

[a] *Department of Chemical and Petroleum Engineering, University of Calgary, Calgary, AB, Canada*
[b] *Department of Molecular and Macromolecular Chemistry, Graduate School of Engineering, Nagoya University, Furo-cho, Chikusa, Nagoya 464-8603, Japan.*
[c] *Nagoya University Venture Business Laboratory, Nagoya University, Furo-cho, Chikusa, Nagoya 464-8603, Japan*
[d] *Canadian Nuclear Laboratories, Chalk River, ON, Canada*
[e] *School of Materials Science, Japan Advanced Institute of Science and Technology, 1-1 Asahidai, Nomi, Ishikawa 923-1292, Japan.*

† **Supplementary Information:** The difference between volumetric and thickness expansion from cycle-to-cycle is present in SI. Fits on GISAXS data (intensity vs scattering vector) are presented. Method to estimate volume fraction from the NR-SLD is presented. Fitting of the NR data and all the fit parameters to validate the selection of model shown in main paper is presented.

SiO_2 [24, 30-31]. In other words, macroscopic properties and likely the microscopic structure of thin Nafion films not only differ from those of the bulk membrane but also are substrate-dependent.

Insofar as the microscopic structure – the ionic domain – is concerned, a hydration-dependent d-spacing derived from the so-called ionomer peak in SAXS data provides an insight on the size of the hydrated domains [22, 36]. For Nafion thin films, the GISAXS measurements have shown anisotropic character (in-plane vs out-of-plane) of the ionomers [22, 30]. Both confinement and interaction with the substrate can induce hydration dependent non-uniform spatial distribution of d-spacing. Although SAXS is a very powerful tool in determining the size of micro-domains, it does not provide information on the spatial distribution of the d-spacings or on their spatial configuration and connectivity. This adds to the complications in correlating the macroscopic changes, i.e. the swelling of films with the changes in the microscopic structural parameter, i.e. the ionic domain related d-spacing. Furthermore, the commonly employed methods for determining the macroscopic hydration property of ionomer thin films, viz., ellipsometry and quartz crystal microbalance (QCM) fundamentally measure different characteristics. Ellipsometry measures overall thickness change of polymers, whereas QCM measures the total mass change. Often the analyses consider that the dry polymer volume and water volume are additive to yield the observed change. Such assumption neglects any changes in the density of the hydrophobic matrix upon water sorption in the hydrophilic ionic domains. Ideally, the volume change (ΔV) determined from swelling measurements should compare with that estimated from mass change. However, if the polymer plasticizes, and its elastic property changes with hydration, swelling based water uptake may not equate to gravimetric mass uptake. A previous study on Nafion thin film coated on Au showed a higher ΔV estimated from mass uptake measured using QCM than ΔV calculated from swelling measurements using ellipsometry [27]. Furthermore, it is unlikely that interfacial water on a realistic (non-atomistic smooth) surface will contribute to the swelling of the ionomer. Our recent NR study has shown that a significant amount of water can be present at the Pt/ionomer interface [34]. As alluded above, NR studies have also shown non-uniform distribution of water through the thickness of the Nafion film [31]. Thus, it may be expected that the number density and/or the size of the hydrated domains may vary across the thickness of the films. Therefore, it is not obvious whether the microscopic parameter (d-spacing) would linearly correlate with the macroscopic parameter (swelling).

The review of the literature reveals that, in general, there has been only a very limited effort to correlate the macroscopic properties of the ionomer thin films with its microscopic structure. So far only one study reports the relationship between the macroscopic and microscopic expansions of thin films on SiO2 where a ~50 nm thin film follows affine behavior i.e. macroscopic expansion 1:1 correlates with microscopic expansion [22]. However, given the significant differences in macroscopic properties of Nafion thin films on SiO2 and on Pt, the microscopic-macroscopic property relationship presented for films on SiO_2 cannot be assumed to be applicable for films on Pt [5, 22].

This study is a first report wherein the hydration behavior of a ~55 nm Nafion thin film on an electrochemically relevant Pt substrate is cross-correlated with multiple techniques – ellipsometry, quartz crystal microbalance, GISAXS, and neutron reflectometry - examining the structure and/or properties at multiple-length scales. Simultaneous measurements of hygro-expansion (by ellipsometry) and mass water uptake (by quartz crystal balance or QCM) on the same sample over a range of relative humidity were carried out. The results demonstrate a systematic difference in water content estimated from the two methods, which may have implications for a majority of the literature data on perfluoro sulfonic acid (PFSA) thin films obtained from ellipsometry. The RH-dependent microscopic structure, viz. the hydrophilic domains from GISAXS and the water distribution using NR were measured. GISAXS results provide evidence of in-plane domain expansion opening up the possibility of in-plane film expansion, which has typically been neglected in the literature. NR measurements show non-uniform distribution of water in the out-of-plane direction, which raises the question about the relevance of using a single-value of d-spacing (derived from the ionomer peak of GISAXS data) to characterize the microscopic structure. Finally, the microscopic (d-spacing) and macroscopic (water volume fraction) hydration parameters are correlated to the structural factor (phase volume/tortuosity or ε/τ) for proton conductivity using conductivity data for ~50 nm Nafion reported in an earlier study [23]. The implications of the hydrated microstructure on electrochemical activity and oxygen transport is also discussed.

II. Experimental

A. Sample preparation

Two different Pt substrates were employed: a Pt-electrode of a QCM crystal (Inficon, USA) and a sputter-coated Pt film on a SiO_2 substrate. A 1.7 wt% dispersion of EW1100 was prepared by adding appropriate amount of iso-propyl alcohol (IPA) to stock solution. The Nafion dispersion was spin coated on the Pt substrates and dried in vacuum for 24 hours at 40 ^oC.

B. Combined QCM-Ellipsometry

An environmental cell was designed to accommodate the QCM holder (details) and to control both RH and temperature. Humidified air was flowed through the cell and desirable RH was obtained by mixing a fully humidified gas stream with a dry gas stream. Upon change in RH direct mass uptake of water in the film was measured as a frequency change (Stanford Research Science Instruments) and simultaneously the change in film thickness was measured using an ellipsometer (M2000, JA, Woollam, USA).

C. RH dependent contact angle

A goniometer is used to measure contact angle at controlled RH using salt solution and temperature in an environmental chamber (Rame Hart Inc., NJ, USA).

D. Water distribution in thin films as determined by NR

Thin films coated on Pt films were employed for NR measurements at the National Research Universal (NRU) reactor at the Canadian Nuclear Laboratories in Chalk River, Canada. Details on the used sample cell can be found elsewhere [37]. Salt solutions were used to maintain specified RH and the cell was immediately exposed to ambient RH every time before the salt solution was changed. A typical NR measurement took 8-12 hours.

E. RH dependent GISAXS

GISAXS measurements were taken with a Rigaku FR-E X-ray diffractometer with an R-AXIS IV two-dimensional (2D) detector and Cu Kα radiation (λ = 1.542 Å). Voltage of 45 kV, current of 45 mA, and irradiation time of 10 min were applied with beam size of approximately 300 μm × 300 μm and camera length of 300 mm. Samples were placed into a humidity-controlled cell with X-ray transparent polyester film (Lumirror) windows. Nitrogen carrier gas

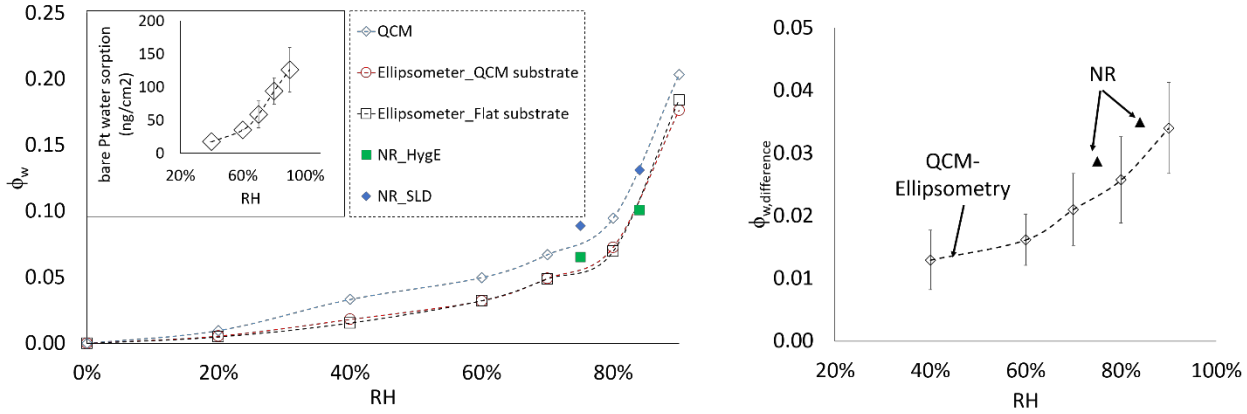

Figure 1. a) Estimated φ_w from QCM, Ellipsometry and NR measurements; NR_Hyge and NR_SLD are volume fractions estimated from NR-data fitted film thickness and SLD, respectively of wet and dry films, inset shows mass of water sorbed by bare Pt. b) The difference between φ_w estimated from QCM and ellipsometry data plotted as a function of RH.

was used as received from the gas cylinder without further dehumidification to control the humidity. X-ray scattering patterns were recorded on an imaging plate (Fujifilm Corp.). The incident angle was chosen as 0.20° – 0.22°. For out-of-plane and in-plane profiles, the integrated regions were taken between -0.5° to +0.5° as 2ϑ from the center (0°) and the width of 1° as 2ϑ, respectively.

III. Result and Discussions

A. Swelling and water mass uptake

Small difference in water volume fraction (φ_w) in ~50 nm Nafion film on gold from mass uptake (QCM) and swelling (ellipsometry) was reported in a previous study co-authored by one of the authors of current study [27]. In the previous work, two separates samples were used for QCM and ellipsometry. Thus, there has been a lingering question whether the observed difference is due to sample to sample variation or a real phenomenon. To eliminate the sample-to-sample variation issues, in this work, humidity-dependent hydration behavior of a ~54 nm thin Nafion film on Pt surface of QCM electrode was simultaneously measured by QCM that yielded mass uptake (Δm, accuracy ± 17 ng/cm^2) and by ellipsometry which yielded swelling (ΔL, accuracy ± 1 Å), respectively. In a separate experiment, using ellipsometry, the swelling of a ~54 nm thin Nafion film on a 10 nm thick Pt/SiO_2/Si substrate was measured as well. Assuming that the hydrophobic matrix density remains unchanged upon hydration of ionic domains, the volume of hydrated ionomer is equal to the volume of dry polymer plus the volume of water sorbed by the ionomer at a given RH. Thus, the mass uptake and swelling can be converted to water volume fraction (φ_w) in the hydrated polymer as reported and compared in Figure 1a. The inset in Figure 1a shows the water uptake on bare Pt substrate as a function of RH. In the case of QCM, to estimate water volume fraction the mass of sorbed water on bare Pt was deducted from total mass of water absorbed by the Nafion thin film.

In a separate experiment, neutron reflectometry measurements on a film of similar thickness was also performed and is discussed in detail in a later section. Data fitting of the NR results yields two parameters – film thickness and the scattering length density (SLD). The thickness and SLD of the dry and the hydrated films independently yield water volume fractions and are denoted as NR-HygE and NR-SLD water volume fraction, respectively and are shown in Figure 1a. The differences in φ_w estimated from three different ionomer coated Pt samples investigated by three different techniques: a) mass uptake from QCM using the Sauerbrey Equation b) swelling from ellipsometry and NR data fitting c) volume fraction from the difference in the SLD of dry and hydrated (wet) films, is quite noticeable. The difference in φ_w from QCM and ellipsometry is denoted by $\varphi_{w,difference}$ and plotted in Figure 1b. Although QCM and ellipsometry derived φ_w were obtained from different areal size examined in the two techniques, viz. 1 cm^2 for QCM and ~ 0.36 cm^2 for ellipsometry, they compare very well with NR-derived volume fractions obtained from the SLD and the thickness (NR SLD φ_w and NR HygE φ_w), respectively. This strongly supports the observation that the differences in water volume fractions obtained from the swelling and water uptake data, even if small, are real and significant. All the equations pertaining to the calculation of water volume fraction are presented in the supplementary information. The changes due to RH cycling is also reported for one sample that was cycled three times between 0% and 90% RH, showing a systematic difference in water volume fractions computed from hygro-expansion and mass uptake analyses for each cycle (Figure S1 of SI), even if the swelling vary slightly from cycle-to-cycle. This further highlights the technique-dependent difference in water content estimation.

Both φ_w and $\varphi_{w,difference}$ increased steadily with RH and a sharp increase in both is observed after 80% RH where φ_w from QCM is almost 10% of the total volume. Evidently, from Figure 1a, most of the water uptake is due to the swelling of the film in the out-of-plane direction, which is expected as film is confined, and strongly interacting with Pt [30]. Even though water uptake in Nafion thin film simultaneously measured from two different methods, the $\varphi_{w,difference}$ can arise from systematic experimental error. On the other hand, such a difference point towards from the real physical possibilities: compression or densification of the hydrophobic backbone, possible in-plane expansion of the film, or the condensation of water in the pores.

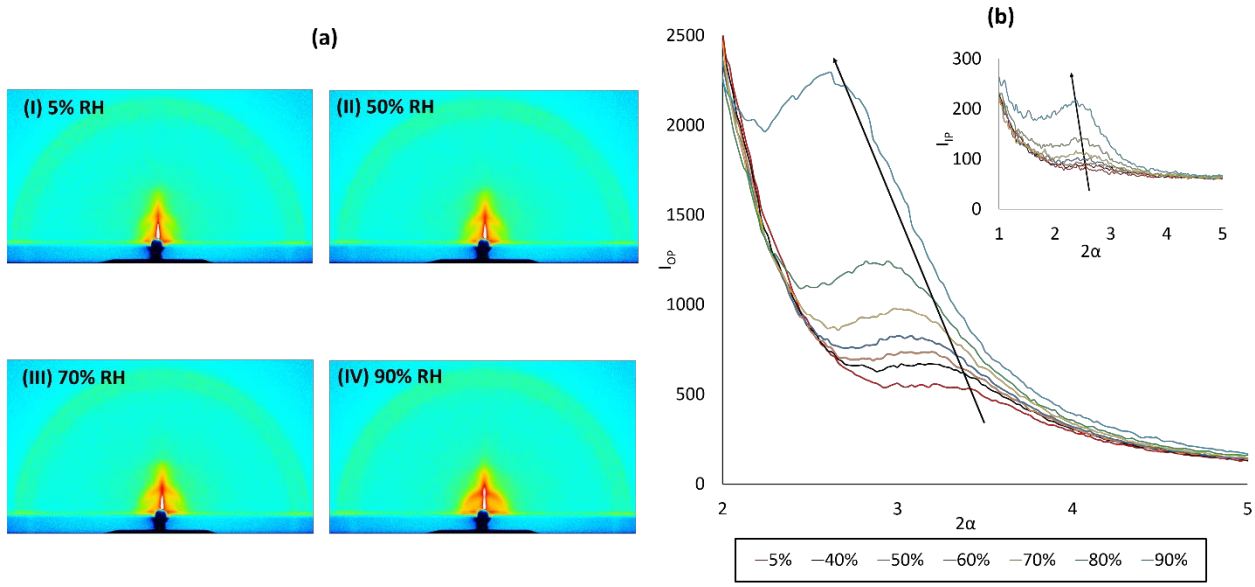

Figure 2. GISAXS measurements for 54 nm Nafion (EW 1100) film on Pt equilibrated at various humidity. a) GISAXS pattern at (I) 5% RH, (II) 50% RH, (III) 70% RH, (IV) 90% RH b) Intensity as a function of scattering vector from 5% RH to 90% RH, inset shows IP intensity vs. scattering vector.

B.Microscopic-macroscopic expansion

To further our understanding of hygro-expansion of the film, we analyzed the GISAXS results to relate micro-structure to macroscopic swelling. RH dependent GISAXS response of the film was measured from 5% to 90% RH; examples of GISAXS patterns are presented in Figure 2a, I-IV. From the 2D profiles both out-of-plane (OP) intensities (I_{op}) and in-plane (IP) intensities (I_{IP}) were derived and plotted against the scattering vector (q, nm^{-1}) in Figure 2b. With increasing RH and as the corresponding water uptake increases, there is both an increase in the scattering intensity and a shift of the scattering peak towards the lower q.

The d-spacing, obtained from the peak position, as a function of RH is plotted in Figure 3. Whereas a discernable change in OP d-spacing with RH is noticeable for the whole range (20-90% RH), the IP d-spacing change was quantifiable only above 60%RH (fits are presented in Figure S2 of SI). Upon extrapolation, the OP d-spacing (2.5 nm) in dry state of Nafion thin film on Pt is very close to the d-spacing (2.7 nm) of dry membrane [21]. Further, at similar water content (λ ~ 7), the OP d-spacing (3.2 nm) of thin film on Pt is 11% lower than the overall d-spacing (3.6 nm) of membrane while matches with OP d-spacing of 50 nm Nafion thin film on SiO_2 [21].

Shift in I_{IP} to lower q with increasing RH indicates that the d-spacing in IP-direction is increasing. Confinement effects and/or strong interaction of the ionomer with the substrate would both result in restricted mobility in the IP direction yet the film is free to expand in OP direction. This could explain the noticeable expansion of OP component of the domains at RH of up to 60% but correspondingly small expansion of IP component. Also, the d-spacing in IP directions are larger than that in the OP direction. Considering these results, it may be deduced that both, confinement and interaction of ionomers with Pt are responsible for the constrained expansion in IP direction at low RHs but once domains are filled with sufficient water, the plasticization of polymer allows IP expansion. d-spacing can increase due to the expansion of the matrix and/or of the water-filled hydrophilic domains. Further, Kusogulu et al., reported increase in nanoscopic swelling of domains in IP direction for Nafion thin film on SiO_2 [21]. In their work, coalescence of IP domains was presented as a hypothesis to explain local swelling of nanoscopic domains. It is also been argued that the $\varphi_{w,difference}$ may arise from in-plane expansion of films [27]. There is a possibility of in-plane expansion due to the microscopic swelling. However, in the absence of a direct evidence, IP domain expansion cannot be used as a concrete proof of in-plane expansion and, by extension, it cannot be established with certainty that $\varphi_{w,difference}$ arises from in-plane expansion.

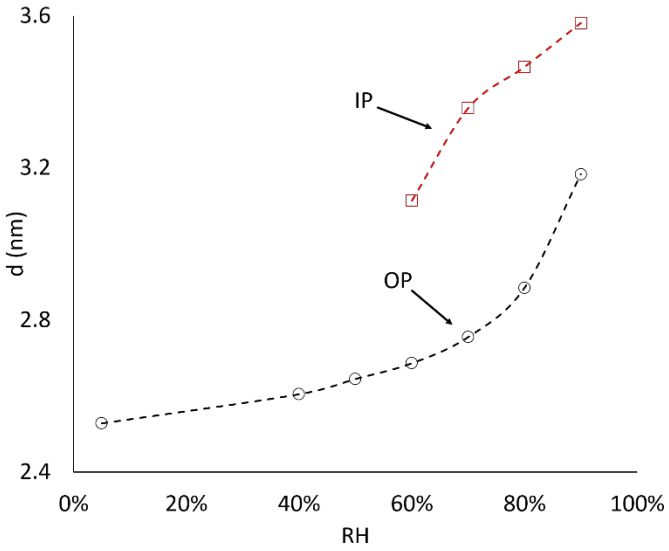

Figure 3. Microscopic and macroscopic swellings as a function of relative humidity for 54 nm thick Nafion (EW1100) coated Pt at 25 oC a) Out-of-plane (OP) and in-plane (IP) d-spacings obtained from analyses of GISAXS data (Figure S2 in SI).

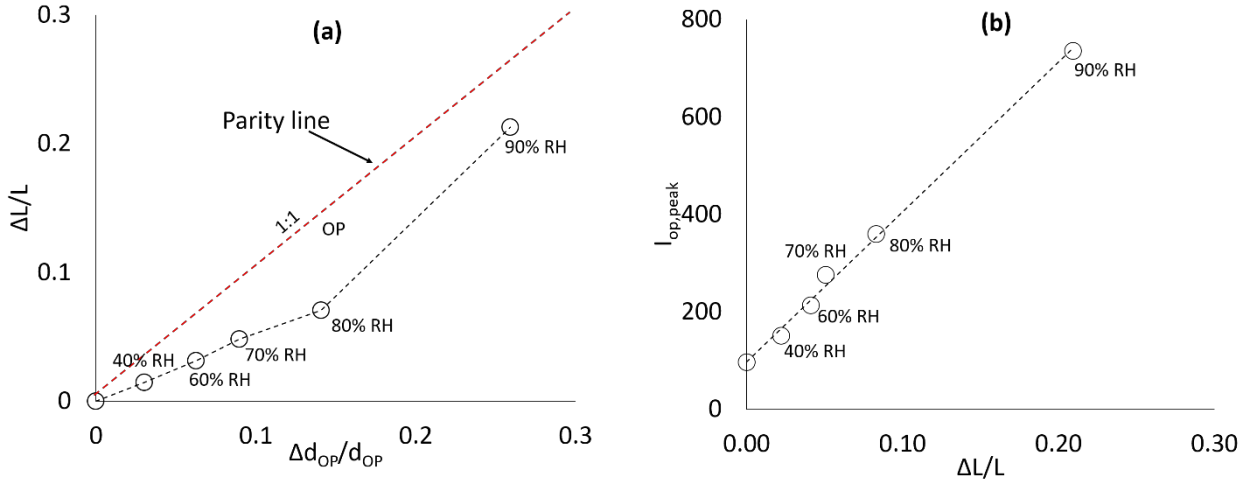

Figure 4. Comparison of macroscopic expansion with microscopic expansion in OP direction b) GISAXS ionic domain OP peak area as a function of swelling or OP macroscopic expansion.

Kreuer and Kusoglu correlated swelling with domain expansion for different PFSA membranes along with various treatments and asserted that their structure is locally flat [11, 21, 36]. However, d-spacing in itself is not sufficient to provide insight on correlation between microscopic structure and macroscopic structure. For instance, membranes and thin films thicker than 100 nm, show non-affine ($\Delta d/d_{dry}$: $\Delta L/L_{dry} \neq 1:1$) behavior meaning local domain expansion does not correlate 1:1 with overall swelling – a clear explanation of this phenomenon is still lacking [11]. Nonetheless, 55 nm thick Nafion thin films on SiO_2 substrates have been reported to exhibit affine behavior. Here, a similar analysis is performed and the relative change of the domain size in OP direction is computed and correlated with the swelling in OP direction (from ellipsometry). To compute Δd, we reference the OP domain size (d_z) at 0%RH estimated by extrapolation of (d_{OP}) versus RH data. The relative changes in domain size plotted against corresponding changes in macroscopic expansion for films are shown in Figure 4a and a non-affine behavior is clearly noted. Up to 80% RH, similar to previously reported data for Nafion membrane and Nafion film thicker than 100 nm on SiO_2 substrate, a linear correlation between $\Delta d_{op}/d_{op,dry}$ and $\Delta L_{op}/L_{dry}$ is noted but the $\Delta d_{op}/d_{op,dry}$:$\Delta L_{op}/L_{dry}$ ratio is ~ 2:1. For RH between 80% and 90%, this ratio is close to 1:1 indicating affine behavior. Compared to membranes and thick ionomer films where polymer mobility is higher than in a film confined to a substrate and possibly strongly interacting with the substrate since sulfonic groups are known to have strong interaction with Pt [33], the domains are expected to be aligned parallel to the Pt [30] and should result in affine behavior but that is definitely not the case. Both macroscopic water volume fraction and microscopic domain size are essentially average quantities and possibly non-uniformly distributed within the confined ionomer thin film. Moreover, a thin film confined to the substrate also has a certain orientation order which changes with RH [28]. Thus, it is not essential that changes in a single microscopic parameter, d-spacing obtained from GISAXS data, may necessarily exhibit affine relationship with macroscopic changes.

The area under I-q Gaussian curve is proportional to the volume fraction of scatterers [36-38] and for a locally flat thin film Gaussian area is expected to be proportional to swelling - which is the case (see Figure 4b). In a homogeneous/isotropic ionomer material, all the ionic domains would have nearly equal water content. Thus, the number of scatterers do not change but their size and correspondingly the volume fraction of the scattering entities increase with increasing hydration. On the other hand, ionomer thin films can be anisotropic and are known to exhibit layered structure with varying water content through the thickness of the film. In other words, the domains may be unequally hydrated. Thus, in essence, the effective number of scatterers will be changing with hydration. An integrated value of intensity with respect of q-vector would account for changes in the number of scatterers.

In our experiments, at 5% RH a small peak has been observed in the q-range typically attributed as the 'ionomer peak' indicating that at least some of the domains may be sufficiently hydrated. With increase in RH, both, the peak intensity and its position are expected to change. The integrated area correlates linearly with macroscopic expansion (ΔL) suggesting that the non-affine behavior of the ionomer film most likely arises from non-uniform spatial distribution of water within the film.

For RH dependent water distribution in the OP direction, we examined the neutron reflectometry (NR) data at 8%, 75%, and 84% in H2O environment. The reflectivity response was fitted with a four-layer model (Table S1 in SI describes the quality of the fit). At dry conditions (8%RH), a single layer with uniform SLD was found to be sufficient to describe the NR response from the Nafion film structure while at higher RHs a multi-layer model, as described below, was needed to fit the data (all the fits with NR data are shown in Figure S3). The corresponding SLD profiles are shown in Figure 5a.

The multi-layer description of the ionomer film comprises of three layers with uniform SLD and two gradient layers with an error function like SLD profile. The layered model comprises: i) an interfacial layer in contact with Pt, which is a mix of water and polymer; the SLD of this layer is lower compare to the SLD of dry (8% RH) film because the SLD of H2O is -0.056 10-5/Å2; ii) an inner layer, which is the driest layer within the film and it SLD approaches that of the dry polymer; iii) a gradient layer wherein the SLD transitions from that of the dry inner layer to that of the wetter outer layer; iv) an outer layer with lowest SLD implying that most of the water is accumulated in this layer; v) a hydrophobic surface layer where SLD approaches that of the SLD of dry layer; noticeably this hydrophobic layer persists even when the film is exposed to RH as high as 88% for

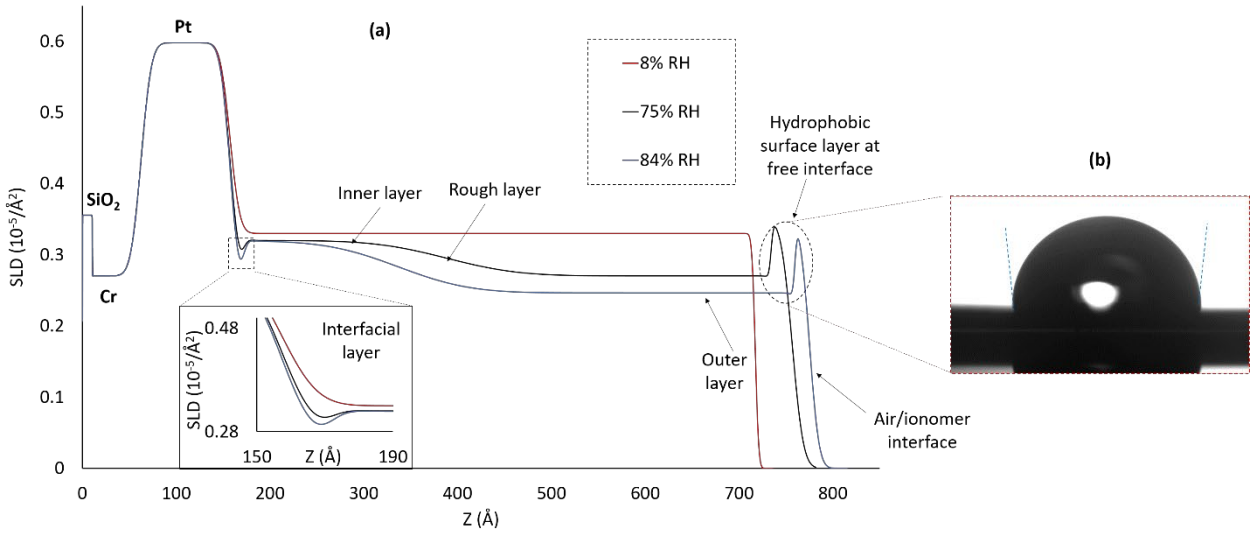

Figure 5. a) SLD profile of Nafion film on Pt at different relative humidity (H_2O environment) at 25 °C b) An image of water contact angle measured at the surface of ionomer at ~88% RH.

24 hours, in Figure 5b, contact angle present a strong evidence of such a surface layer.

The overall physical description of the Nafion thin film is supported by external evidences: 1) water sorption at bare Pt is an indirect evidence of water at Pt-ionomer interface, 2) $\varphi_{w,difference}$ estimated from NR model based SLD and swelling is similar to $\varphi_{w,difference}$ from QCM and ellipsometry, and 3) presence of hydrophobic skin layer from model also described by the contact angle measurements. The hydrophobic surface of Nafion is well known and is discussed in a recent article by Karan [5]. There is evidence of skin layer from GI-SAXS and GI-XRD studies of Nafion films [40-41].

Using Equation S5 of SI SLDs were converted to water volume fraction. As RH increases from 75% to 84%, the φw in the 1.4 nm thick interfacial layer at the buried interface (see SLD profile in Figure 5a) increases from 20% to 26% indicating humidity-dependent interfacial water. Beyond the interfacial layer, a dry layer exists near the interface with φw ~ 3% at both RHs however the thickness of the dry inner layer reduces from 26 nm to 17 nm as RH increases from 75% to 84%, and the roughness of the inner layer remains the same, 6 nm which translates to a 24 nm thick gradient layer. In similar fashion, the thickness of the wet outer layer increases from 30 nm to 42.5 nm whereas φw increases slightly from ~15% to ~21%. In either cases, a rough hydrophobic surface layer or skin layer persists at 75% RH and 84% RH. In a separate experiment using a special environmental chamber, similar films on Pt were exposed for 18 hours to 75% and 84% RH (i.e., similar to the conditions of the NR experiments) and found the water contact angle of ~90o (see an image in Figure 5b). It is quite intriguing that the nature of the surface is independent of RH. In fact, Kawamoto et al., reports a similar RH independent surface layer for ionomers coated on a Si substrate [39]. Even though NR measurements could not be performed at all the RHs, it provides sufficient evidence of spatial distribution of water within the ionomer coated on Pt. Thus, non-affine behavior is likely to originate from spatial distribution of the water. To elaborate, one of the reasons put forth for suppressed water uptake in thin films compared to thicker films and membranes is the idea of higher elastic modulus of the polymer for thinner films [5, 16]. Due to the higher elastic modulus, higher mechanical forces exerted by the hydrophobic matrix counteracts the chemical force for hydration resulting in a lower water uptake. A gradient in elastic modulus can be expected for Nafion films on platinum. The polymer near the substrate has arguably higher elastic modulus due to strong interaction with the Pt substrate compared to the polymer away from the Pt/ionomer interface. Thus, the gradient in water distribution is most likely to originate from the gradient in the elastic modulus from the buried interface to the surface of the ionomer.

C. Conductivity-structure correlation of ionomer thin film on Pt

Ono et al. have reported conductivity measurements (σ in S/cm) of ~50-55 nm thin film on Pt in an earlier study [23]. The water content, λ (# of water molecules/ sulfonic molecule) of a 55 nm film can be deduced from the mass uptake measured by QCM in the present work:

$$\lambda = \frac{M_{RH,ion} - M_{dry,ion}}{M_{dry,ion}} \cdot \frac{EW \cdot \rho_w}{\rho_{ion} \cdot M_w} \qquad (1)$$

where, $M_{RH,ion}$ is the RH dependent mass of the ionomer film, $M_{dry,ion}$ is mass of the dry ionomer film, *EW* is the equivalent weight, ρ_w the density of water, ρ_{ion} the density of ionomer, and M_w is the molecular weight of water.

It can be noted from the data in Figure 6a that σ increases by two orders of magnitude from 40% to 90% RH and λ increases steadily till 80% RH and then sharply between 80% RH and 90% RH. It is common to correlate the proton conductivity σ with λ. It is obvious from Figure 6b that at λ < 4, conductivity is very sensitive to water content. For instance, λ increases by 2 between 40% and 80% RH but σ increases by orders of magnitude and then four times till λ~8. It should be noted that λ is an average value computed from the overall water volume or mass fraction and does not take into account the OP water distribution. These average lambda values indicate the average local chemical environment of the sulfonic groups i.e. amount of water molecules attached to a sulfonic group and can dictate the water transport mechanism.

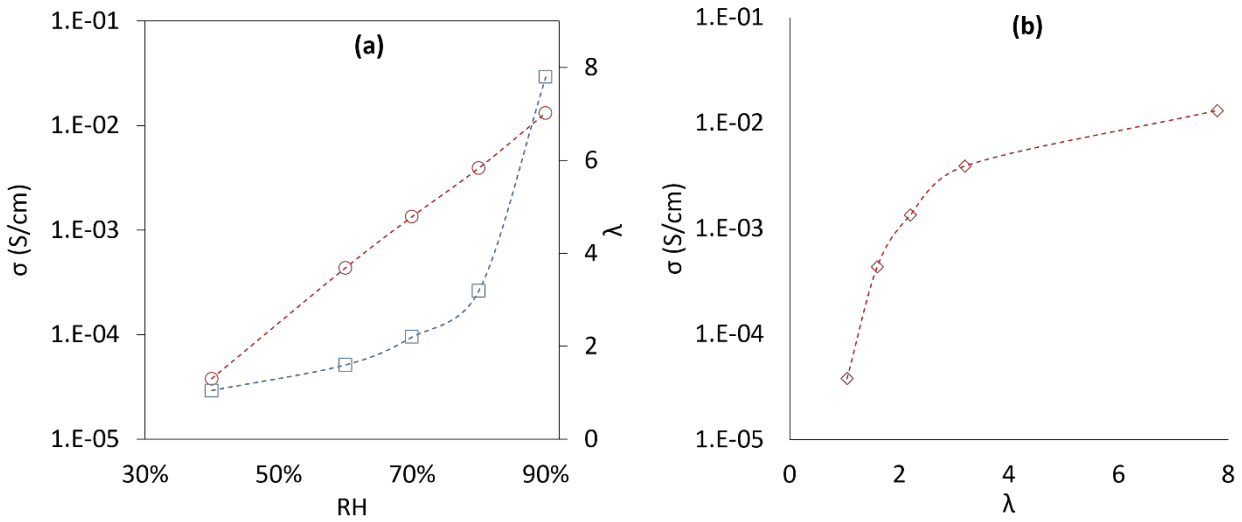

Figure 6. a) Conductivity (red_circle) [23] and water content (blue_squares) [This Work] of ~50-55 nm ionomer thin film on Pt at 30 °C b) Conductivity as a function of water content at 30 °C.

For PFSA membranes, Kusoglu et al., identified an empirical relationship among conductivity (σ), water content (λ), and domain spacing (*d*), and that is $\sigma \propto {}^{\lambda}/_{d}$ [21]. However, by accounting structural properties such as volume fraction of water-filled domains proton transport (ε) and tortuosity of pathways (τ) for the long-range transport of protons, the generic form of conductivity of protons in an ionomer thin film or membrane in terms of proton concentration (C_{H^+}) and proton mobility (μ_{H^+}) is commonly expressed as:

$$\sigma = [C_{H^+}\mu_{H^+}][{}^{\varepsilon}/_{\tau}] \qquad (2)$$

Choi et al. developed a model to compute the proton conductivity of Nafion membrane [42]. In particular, their model accounted for the water content (λ) dependent mobility and concentrations of protons by considering surface and bulk (comprising Grothuss and free water) transport within the connected network of hydrophilic ionic domains. The commonly used epsilon-tau (ε/τ) model was adopted considering the composite nature of the ionomer accounting for the volume of the conducting phase (ε) and tortuous pathways of the conducting phase (τ). The conductivity equation proposed by Choi et al [42] is shown below:

$$\sigma = (\varepsilon/\tau) \cdot \left[\frac{F^2}{RT}\left(D^{\Sigma}_{H^+}C^{\Sigma}_{H^+} + D^{G}_{H^+}C_{H^+} + \frac{D^{W}_{H^+}C_{H^+}}{1+\delta_c}\right)\right] \qquad (3)$$

where, F is the Faraday constant, R the universal gas constant, T the temperature, $D^{\Sigma}_{H^+}$ the surface proton diffusivity, $D^{G}_{H^+}$ the Grothuss proton diffusivity, $D^{W}_{H^+}$ the vehicular proton diffusivity, $C^{\Sigma}_{H^+}$ the concentration of surface protons, C_{H^+} the concentration of exchanged protons, and δ_c is the diffusion coefficient ratio. Here, the term within square brackets can be thought of the intrinsic conductivity of the protons within the ionic domains and is the function of λ only. It can be argued that the differences in the observed conductivity between a thin film and bulk ionomer at a given λ is attributable to the microstructural parameters (ε/τ). The parameter ε is equivalent to φ_w. Below φ_w ~ 0.2, Kreuer et al., found highly suppressed proton conductivity but almost similar to water diffusivity in Nafion membrane which indicates that the vehicular mechanism dominates the proton transport in membranes [43]. For the conductivity measurements reported on 50 nm Nafion film by Nagao group, the water volume fraction (φ_w) is below 0.2. Hence, vehicular mechanism is assumed as primary mechanism of proton transport, which simplifies the form of Equation 3 to:

$$\sigma = (\varepsilon/\tau)\left[\frac{F^2}{RT}\left(\frac{D^{W}_{H^+}C_{H^+}}{1+\delta_c}\right)\right] \qquad (4)$$

Kreuer et al. compared the microstructural domain size, water diffusivity, and proton conductivity among polyaryl hydrocarbon and Nafion membranes [43, 44]. In their work, Polyphenylene and Nafion membrane exhibited comparable diffusivity at similar λ but hydrophilic domains in polyphyenylene were measured to be smaller than Nafion – indication of weak correlation between domain size and intrinsic conductivity. Yet, at a similar volume fraction proton conductivity of polyphenylene membranes were much lesser than Nafion [43]. Similarly, sulfonated-poly ether ketone membrane with much smaller domain size than Nafion, which result in highly tortuous and dead end domains, showed relatively much lower water diffusivity and conductivity at same volume fraction [44]. Observations from these papers are indicative of domain size relevance to the structural parameters. Therefore, as the film expands, both, an increase in domain size and water volume fraction lead to the development of more proton conducting pathways, and tortuosity is expected to fall. Linear relationship between structural factors (ε/τ) computed from Equation 3 with product of water volume fraction and domain expansion $\varphi_w \Delta d_{op}$ is identified (Figure 7). Furthermore, since, φ_w is equal to ε, the tortuosity of proton-conducting domains can be computed. It is found that the tortuosity is inversely proportional to the domain expansion (see inset in Figure 7).

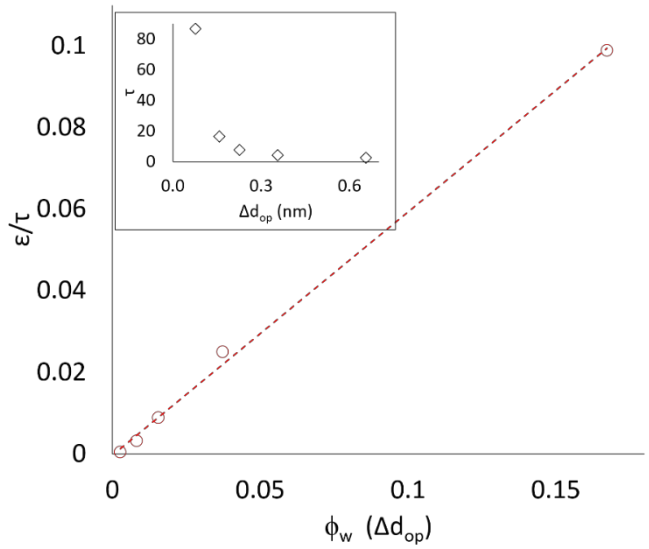

Figure 7. Comparison between structural factors and product of water volume fraction and domain expansion, inset shows tortuosity against domain expansion.

D. Implications to oxygen transport resistance and Pt poisoning

Oxygen transport resistance across the ionomer thin film and Pt poisoning owing to adsorption of sulfonic groups are relevant to the performance of fuel cell. Recent report from Morimoto's group have clearly pointed out that Pt poisoning occurs mainly due to the adsorption of sulfonic groups at Pt site. The degree of adsorption or poisoning strongly depends on the amount of interfacial water (water at the Pt/ionomer interface) which increases as RH increases resulting in more sulfonic group desorption [45]. Evidently, NR data from the present study shows that the φ_w at the interface increases from 20% to 26% as RH increases from 75% to 84% and in a previous NR study from our group [33], at 97% RH two monolayers of water at Pt-ionomer interface separating ionomer from Pt was measured. Consequently, water has a major role in reducing the Pt poisoning, mechanism of which is replacement of sulfonate groups by water.

In another study from Morimoto's group, in an ex-situ experiment it was found that the estimated interfacial resistance for oxygen transport and diffusivity of oxygen through thin film decreases with RH. From 30% RH to 90% RH, oxygen diffusivity increases by three times and interfacial resistance to oxygen transport decreases by 20% [13]. Bulk oxygen diffusion resistance should be related to bulk microstructure and interfacial resistance should be related to near interface structure. Oxygen is transported through two pathways: a) free volume in the backbone and b) hydrophilic domains. It is evident from the data on hydrophilic domain size that increase in oxygen diffusivity must be result of hydrophilic domain expansion (see Table-1). Similarly, as Pt-ionomer interface hydrates the free volume near interface increase and results in lower interfacial resistance for oxygen transport. However, layer at the free interface or surface layer remains hydrophobic, meaning water cannot easily breakthrough the hydrophobic backbone which raises the question *how oxygen is transported at the free interface*?

Table 1. Comparison of oxygen transport resistance across the Nafion thin film coated on Pt and domain size in OP and IP directions.

RH (%)	O_2 diffusion at 40 °C [13]		d-spacing [This work]	
	Inner resistivity (10^{14} s.m.Pa/mol)	Interfacial Resistance (10^6 s.m^2.Pa/mol)	d_{OP} (nm)	d_{IP} (nm)
30	3.4	10	2.55	-
40	-	-	2.6	-
60	1.9	8.8	2.7	3.2
90	1.1	7.8	3.2	3.6

VI. Conclusions

A finite difference in water volume fraction in ionomer thin films computed from the difference in swelling from ellipsometry and mass uptake from QCM. The correlation between hydrophilic domain expansion and swelling in OP direction yielded non-affine behaviour of thin films on Pt. The origin of non-affine behaviour is attributed to the water distribution within the ionomer thin film, evidence of which was provided by RH dependent water distribution determined by NR.

The proton conductivity-water uptake of ionomer thin film on Pt was analysed in terms of structural parameters: water volume fraction and domain size. In the vehicular transport dominated regime ($\varphi w < 0.2$), we identified that the tortuosity of ionomers is inversely proportional to the hydrophilic domain size. Further, implications of RH dependent water distribution from NR and hydrophilic domain size on oxygen diffusion and ORR activity was discussed. In bulk ionomers, increase in domain size very well relates with increase in oxygen diffusivity with RH. Similarly increase in free volume with RH at Pt-ionomer interface could be the underlying cause of increase in oxygen diffusivity with RH at the Pt-ionomer interface. In addition, increase in water content at the Pt-ionomer interface with RH also promotes desorption of sulfonic group thereby increases ORR activity at Pt-ionomer interface.

Conflicts of interest

Authors declare no conflict of interests.

Acknowledgements

Authors are grateful to Dr. K.D. Kreuer (Max Planck Institute for Solid State Research, Stuttgart, Germany) for the discussion on interpretation of the GISAXS data presented in this work. The financial assistance for this work was provided by the Natural Sciences and Engineering Research Council of Canada (NSERC) for KK's Discovery Grant and UNS's Post-Doctoral Scholarship funds from Canada First Research Excellence Funds (CFREF). We also acknowledge the technical support from Canadian Nuclear Laboratories (CNL), Chalk River, Canada for our Neutron Reflectometry measurements, especially the technical assistance from Carl Neggers (CNL, Chalk River, Canada). We are also grateful to Dr. Milana Trifkovic postdoc Dr. Mohammed Elsutohy to help us with fluorescence microscopy.

References

1. M.S Wilson, S. Gottesfeld. Thin-film catalyst layers for polymer electrolyte fuel cell electrodes. Journal of applied Electrochemistry, 1992, 22, 1-7.
2. Q. Luo, H. Zhang, J. Chen, P Qian, Y. Zhai. Modification of Nafion Membrane Using Interfacial Polymerization for Vanadium Redox Flow Battery Applications. Journal of Membrane Science, 2008, 311, 98-103.
3. C.D. Feng, S.L. Sun, H. Wang, C.U. Segre, J.R. Stetter. Humidity Sensing Properties of Nafion and Sol-gel Derived SiO2/Nafion Composite Thin Films. Sensors and Actuators B: Chemical, 1997, 40, 217-222.
4. S.A. Grigoriev, V.I. Porembsky, V.N. Fateev. Pure Hydrogen Production by PEM Electrolysis for Hydrogen Energy. International Journal of Hydrogen Energy, 2006, 31,171-175.
5. K. Karan. Interesting Facets of Surface, Interfacial, and Bulk Characteristics of Perfluorinated Ionomer Films. Langmuir, 2019.
6. K.Karan. Recent Advances in Materials, Microstructural Characterization, and Modeling. Current Opinions in Electrochemistry, 2017, 5, 27-35.
7. Y. Sone, P Ekdunge, D. Simonsson. Proton Conductivity of Nafion 117 as Measured by a Four-electrode AC Impedance Method. Journal of the Electrochemical Society, 1996, 143, 1254-1259.
8. T.A. Zawodzinski, C. Derouin, S. Radzinski, R.J. Sherman, V.T. Smith, T.E. Springer, S. Gottesfeld. Water Uptake by and Transport Through Nafion® 117 Membranes. Journal of the electrochemical society, 1993, 140, 1041-1047.
9. K.C. Neyerlin, W. Gu, J. Jorne, A. Clark, H.A. Gasteiger. Cathode catalyst utilization for the ORR in a PEMFC analytical model and experimental validation. Journal of The Electrochemical Society, 2007, 154, B279-B287.
10. D. Chen, A. Kongkanand, J. Jorne. Proton Conduction and Oxygen Diffusion in Ultra-Thin Nafion Films in PEM Fuel Cell: How Thin?. Journal of The Electrochemical Society, 2019, 166, F24-F33.
11. A. Kusoglu, A.Z. Weber. New Insights into Perfluorinated Sulfonic-acid Ionomers. Chemical Reviews, 2017, 117, 987-1104.
12. K.A. Mauritz and R.B. Moore. State of understanding of Nafion. Chemical reviews, 2004, 104, 4535-4586.
13. K. Kudo, R. Jinnouchi, and Y. Morimoto. Humidity and temperature dependences of oxygen transport resistance of Nafion thin film on platinum electrode. Electrochimica Acta, 2016, 209, 682-690.
14. V. Ozhukil Kollath, Y. Liang, F.D. Mayer, X. Ma, C. Korzeniewski, and K. Karan. Model-Based Analyses of Confined Polymer Electrolyte Nanothin Films Experimentally Probed by Polarized ATR–FTIR Spectroscopy. The Journal of Physical Chemistry C, 2018, 122, 9578-9585.
15. Y. Nagao. Highly oriented sulfonic acid groups in a Nafion thin film on Si substrate. The Journal of Physical Chemistry C, 2013, 117, 3294-3297.
16. K.A. Page, A. Kusoglu, C.M. Stafford, S. Kim, R.J. Kline, and A.Z. Weber. Confinement-driven increase in ionomer thin-film modulus. Nano letters, 2014, 14, 2299-2304.
17. D.K. Paul, A. Fraser, and K. Karan. Towards the understanding of proton conduction mechanism in PEMFC catalyst layer: Conductivity of adsorbed Nafion films. Electrochemistry Communications, 2011, 13, 774-777.
18. D.K. Paul, R. McCreery, and K. Karan. Proton transport property in supported Nafion nanothin films by electrochemical impedance spectroscopy. Journal of The Electrochemical Society, 2014, 161, F1395-F1402.
19. D.K. Paul and K. Karan. Conductivity and wettability changes of ultrathin Nafion films subjected to thermal annealing and liquid water exposure. The Journal of Physical Chemistry C, 2014, 118, 1828-1835.
20. H.K. Shim, D.K. Paul, and K. Karan, K. Resolving the contradiction between anomalously high water uptake and low conductivity of nanothin Nafion films on SiO2 substrate. Macromolecules, 2015, 48, 8394-8397.
21. A. Kusoglu, T.J. Dursch, A.Z. Weber. Nanostructure/Swelling Relationships of Bulk and Thin-Film PFSA Ionomers. Advanced Functional Materials, 2016, 26, 4961-4975.
22. A. Kongkanand. Interfacial water transport measurements in Nafion thin films using a quartz-crystal microbalance. The Journal of Physical Chemistry C, 2011, 115, 11318-11325.
23. Y. Ono, and Y. Nagao. Interfacial structure and proton conductivity of Nafion at the Pt-deposited surface. Langmuir, 2015, 32, 352-358.
24. C. Zhang, M. Davies and K. Karan. Probing interfacial interactions of nafion ionomer: Thermal expansion of nafion thin films on substrates of different hydrophilicity/hydrophobicity. Journal of Polymer Science Part B: Polymer Physics, 2019, 57, 343-352.
25. S.C. DeCaluwe, P.A. Kienzle, P. Bhargava, A.M. Baker and J.A. Dura. Phase segregation of sulfonate groups in Nafion interface lamellae, quantified via neutron reflectometry fitting techniques for multi-layered structures. Soft Matter, 2014, 10, 5763-5776.
26. S.C. DeCaluwe, A.M. Baker, P. Bhargava, J.E. Fischer, and J.A, Dura. Structure-property relationships at Nafion thin-film interfaces: Thickness effects on hydration and anisotropic ion transport. Nano energy, 2018, 46, 91-100.
27. A. Kusoglu, D. Kushner, D.K. Paul, K. Karan, M.A. Hickner, A.Z. Weber. Impact of Substrate and Processing on Confinement of Nafion Thin Films. Advanced Functional Materials, 2014, 24, 4763-4774.
28. M. Tesfaye, D.I. Kushner, and A. Kusoglu. Interplay between Swelling Kinetics and Nanostructure in Perfluorosulfonic Acid Thin-Films: Role of Hygrothermal Aging. ACS Applied Polymer Materials, 2019.
29. M. Tesfaye, A.N. MacDonald, P. Dudenas, A. Kusoglu, and A.Z. Weber. Exploring substrate/ionomer interaction under oxidizing and reducing environments. Electrochemistry Communications, 2018, 87, 86-90.
30. D.I. Kushner, A. Kusoglu, N.J. Podraza, and M.A. Hickner. Substrate-Dependent Molecular and Nanostructural Orientation of Nafion Thin Films. Advanced Functional Materials, 2019, 1902699.
31. J.A. Dura, V.S. Murthi, M. Hartman, S.K. Satija, C.F. Majkrzak. Multilamellar Interface Structures in Nafion. Macromolecules, 2009, 42, 4769-4774.
32. S. Ueda, S.Koizumi, A. Ohira, S. Kuroda, H. Frielinghaus. Grazing-incident Neutron Scattering to Access Catalyst for Polymer Electrolyte Fuel Cell. Physica B: Condensed Matter, 2017.

33. U.N. Shrivastava, H. Fritzsche, and K. Karan. Interfacial and Bulk Water in Ultrathin Films of Nafion, 3M PFSA, and 3M PFIA Ionomers on a Polycrystalline Platinum Surface. Macromolecules, 2018, 51, 9839-9849.
34. Y. Ogata, D. Kawaguchi, N.L. Yamada, and K. Tanaka. Multistep thickening of Nafion thin films in water. ACS Macro Letters, 2013, 2, 856-859.
35. I. Yagi, K. Inokuma, K.I. Kimijima, H. Notsu. Molecular Structure of Buried Perfluorosulfonated Ionomer/Pt Interface Probed by Vibrational Sum Frequency Generation Spectroscopy. The Journal of Physical Chemistry C, 2014, 118, 26182-26190.
36. K.D. Kreuer, G. Portale. A Critical Revision of the Nano-morphology of Proton Conducting Ionomers and Polyelectrolytes for Fuel Cell Applications. Advanced Functional Materials, 2013, 23, 5390-5397.
37. T.A. Harroun, H. Fritzsche, M.J. Watson, K.G. Yager, O.M. Tanchak, C.J. Barrett, J Katsaras. Variable Temperature, Relative Humidity (0%–100%), and Liquid Neutron Reflectometry Sample Cell Suitable for Polymeric and Biomimetic Materials. Review of Scientific Instruments, 2005, 76, 065101.
38. K. Vegso, P. Siffalovic, M. Weis, M. Jergel, M. Benkovicova, E. Majkova, L. Chitu, Y. Halahovets, S. Luby, I. Capek, and A. Satka. In situ GISAXS monitoring of Langmuir nanoparticle multilayer degradation processes induced by UV photolysis. physica status solidi (a), 2011, 208, 2629-2634.
39. T. Kawamoto, M. Aoki, T. Kimura, T. Mizusawa, N.L. Yamada, J Miyake, K. Miyatake, and J. Inukai. In-plane distribution of water inside Nafion® thin film analyzed by neutron reflectivity at temperature of 80° C and relative humidity of 30%–80% based on 4-layered structural model. Japanese Journal of Applied Physics, 2019, 58, SIID01.
40. J. Tang, W. Yuan, J. Zhang, H. Li, Y. Zhang, Y., 2013. Evidence for a crystallite-rich skin on perfluorosulfonate ionomer membranes. RSC Advances, 2013, 3, 8947-52.
41. M. Bass, A. Berman, A. Singh, O. Konovalov, and V. Freger. Surface-induced micelle orientation in Nafion films. Macromolecules, 2011, 44, 2893-99.
42. P. Choi, N.H. Jalani, and R. Datta. Thermodynamics and proton transport in Nafion II. Proton diffusion mechanisms and conductivity. Journal of the electrochemical society, 2005, 152, E123-E130.
43. C.C. De Araujo, K.D. Kreuer, M. Schuster, G. Portale, H. Mendil-Jakani, G. Gebel, and J. Maier. Poly (p-phenylene sulfone) s with high ion exchange capacity: ionomers with unique microstructural and transport features. Physical Chemistry Chemical Physics, 2009, 11, 3305-3312.
44. K.D. Kreuer. On the development of proton conducting polymer membranes for hydrogen and methanol fuel cells. Journal of membrane science, 2001, 185, 29-39.
45. K. Kodama, R. Jinnouchi, T. Suzuki, H. Murata, T. Hatanaka, and Y. Morimoto. Increase in Adsorptivity of Sulfonate Anions on Pt (111) Surface with Drying of Ionomer. Electrochemistry Communications, 2013, 36, 26-28.